Crystal structure of the synergistic antibiotic pair, lankamycin and lankacidin, in complex with the large ribosomal subunit

Matthew J. Belousoff[a], Tal Shapira[a], Anat Bashan[a], Ella Zimmerman[a], Haim Rozenberg[a], Kenji Arakawa[b], Haruyasu Kinashi[b], and Ada Yonath[a,1]

[a]Department of Structural Biology, Weizmann Institute of Science, Rehovot, 76100, Israel; and [b]Department of Molecular Biotechnology, Graduate School of Advanced Sciences of Matter, Hiroshima University, Higashi-Hiroshima 739-8530, Japan

Contributed by Ada Yonath, December 23, 2010 (sent for review November 20, 2010)

The structures of the large ribosomal subunit of *Deinococcus radiodurans* (D50S) in complex with the antibiotic lankamycin (3.2 Å) and a double antibiotic complex of lankamycin and lankacidin C (3.45 Å) have been determined, in continuation of previous crystallographic studies on lankacidin-D50S complex. These two drugs have been previously reported to inhibit ribosomal function with mild synergistic effect. Lankamycin, a member of the macrolide family, binds in a similar manner to erythromycin. However, when in complex with lankacidin, lankamycin is located so that it can form interactions with lankacidin in the adjacent ribosomal binding site. When compared to the well-documented synergistic antibiotics, Streptogramins A and B, the pair of lankacidin and lankamycin bind in similar sites, the peptidyl transferase center and nascent peptide exit tunnel, respectively. Herein, we discuss the structural basis for antibiotic synergism and highlight the key factors involved in ribosomal inhibition.

protein exit tunnel | ribosomes

The ribosome is the universal biomacromolecular multicomponent assembly that translates the genetic code into proteins. It consists of two unequally sized subunits that act together in protein biosynthesis. Decoding and mRNA transit take place on the small subunit, whereas the large subunit provides the machinery for peptide bond formation, nascent protein chain elongation, and its protection.

As a key player in translation, the ribosome is targeted by many antibiotics, all of which impair its function and lead to inviable cells. Simultaneously with the advent of the high-resolution structures of the ribosome, the target sites of antibiotic binding and inhibition have been located and described in detail (1). Furthermore, the crystallographic information has provided enlightenment to mechanisms for antibiotics function and resistance, despite minor structural differences (2) observed in different studies by investigating crystal structures obtained under conditions barely mimicking pathogen–antibiotics relations (e.g., the ribosomes from *Thermus thermophilus* that normally grows at temperatures that cause disintegration of the antibiotics, namely >75 °C; the entire ribosome from *Escherichia coli* that was crystallized without its mRNA and tRNA substrates, thus representing an artificial functional state; the ribosomes from the archaeon *Haloarcula marismortui* that grows at very high salt consecrations, namely ∼3 M KCl, thus cannot exist within human or animal cells and contain features representing eukaryotes rather than the pathogenic eubacteria).

Although ribosomal interfering antibiotics have been in clinical use since the 1950s, rapid resistance, cross-resistance, and drug toxicity drive the need for new treatments for bacterial infection. A potential way to overcome some of the resistance issues is to use pairs of small molecules that inhibit synergistically the ribosome in two different positions. Synercid™, a pair of semisynthetic streptogramins (namely Quinupristin/Dalfopristin, Fig. 1) is currently used as a synergetic pair against Gram-positive resistant strain, such as methicillin-resistant *Staphylococcus aureus* (MSRA) and vancomycin-resistant *Enterococcus faecium* (VREF) (3, 4). Since its clinical approval by the US Food and Drug Administration (FDA) in 1999, this drug combination suffers some resistance by MSRA (5, 6). The synergistic effect of the streptogramins is driven by the streptogramin A (i.e., Dalfopristin) member, which upon binding to the 50S subunit significantly increases the K_a of the streptogramin B (i.e., Quinupristin) component (7).

Lankamycin (LM) and lankacidin C (LC) (Fig. 1) are another pair of antibiotics that are produced by a single organism, *Streptomyces rochei*. Their genes for production are harbored in a large plasmid pSLA2-L (8–10). This dual production hints that their mode of action may also be synergistic. Our previous studies have indicated moderate synergism in their ability to inhibit cell growth as well as cell-free translation (11) and demonstrated that both of these antibiotics bind to 50S ribosomal subunit.

LC, a 17-membered conjugated macrocycle, bridged by a 6-membered lactone, binds in the peptidyl transferase center (PTC) in the 50S subunit (11). LM, a member of the macrolide family, differs from erythromycin in its substituent groups on the macrolactone ring, as well as the two deoxysugars at the C-3 and C-5 positions. However, as these differences are rather modest, it was assumed that LM should bind to the ribosome at the nascent protein exit tunnel in similar position and mode as erythromycin. Interestingly, although LM and LC are able to bind simultaneously, erythromycin disrupts the binding of LC (11).

To obtain a clearer understanding as to the mechanism of synergism of ribosomal inhibition by LM and LC, we determined the three dimensional crystal structures of the complexes of 50S subunit of *Deinococcus radiodurans* (D50S) with LM (LM-D50S) and LM/LC (LM/LC-D50S). This ribosome was shown to serve as an excellent model for eubacterial ribosomes, including bacterial pathogens, and compared them to the structure of the (LC-D50S) complex that has been recently reported (11).

Results

Complete sets of X-ray diffraction data were collected for the D50S complexes with LM-D50S and with both LM and LC (LM/LC-D50S) to a maximum resolution of 3.2 and 3.45 Å, respectively. Using isomorphous replacement to obtain initial phases, clear electron density was observed for the binding sites

Author contributions: A.B., M.B., and A.Y. designed research; M.B., T.S., E.Z., and H.R. performed research; K.A. and H.K. contributed new reagents/analytic tools; M.B., T.S., A.B., E.Z., H.R., and H.K. analyzed data; and M.B., A.B., and A.Y. wrote the paper.

The authors declare no conflict of interest.

Freely available online through the PNAS open access option.

Data deposition: The crystallography, atomic coordinates, and structure factors have been deposited in the Protein Data Bank, www.pdb.org [PDB ID codes 3PIO (D50S-LM) and 3PIP (D50S-LC/LM)].

[1]To whom corrrespondence should be addressed. E-mail: ada.yonath@weizmann.ac.il.

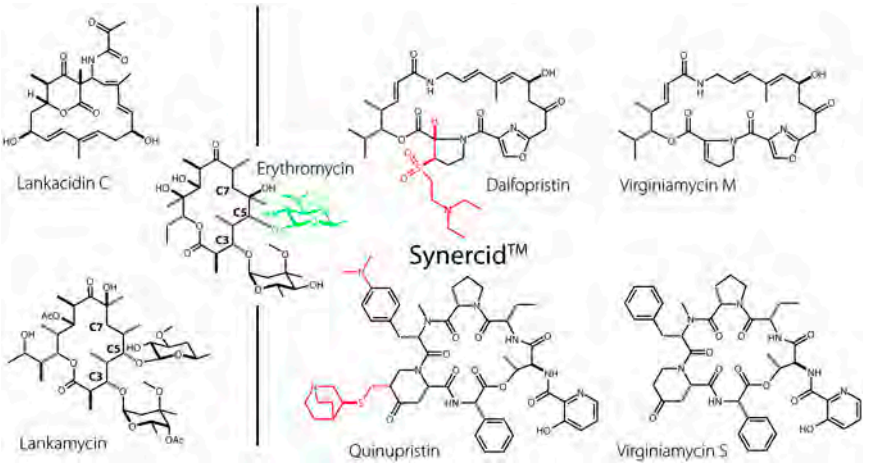

Fig. 1. Chemical structure of ribosomal interfering antibiotics. The desosamine amino sugar of erythromycin, which is replaced by a D-chalcose moiety in Lankamycin, is shown in green. The chemical differences between Synercid™ and the Virginiamycin pair is shown in red.

of LM in LM-D50S and LM and LC in LM/LC-D50S, allowing unambiguous determination of the binding sites of the antibiotics (Fig. 2).

LM-D50S Binding Site. The binding site of LM in the 50S subunit is located at the nascent protein exit tunnel near its entrance. In its binding site LM makes contacts with rRNA nucleotides and not with any r proteins. It forms hydrogen bond contacts between the chalcose sugar and A2058 (*E. coli* numbering used throughout text), the ketone on C-9 and 2′-OH on A2058, and a bridging polar contact between the hydroxyl pendant of C-13 and the ribose sugar of C2611 (Fig. 3*A*). The other contacts it makes with the ribosome are hydrophobic interactions with A2059, A2062, G2505, U2506, C2510, and C2611, completing the binding pocket for LM.

Binding of LM causes a significant change in position of the flexible nucleotide A2062 (important in other synergetic antibiotic interactions; see below) away from the antibiotic (compared to the unbound conformation). Presumably this is due to the steric hindrance of the methyl group C-6 of the macrolide ring, which would be in close contact with the exocyclic amine of A2062. This base movement causes a slight change in the conformation of the nucleobases surrounding A2062. Interestingly it is A2062 that forms a significant hydrogen bond with a related macrolide erythromycin (Ery) between the hydroxyl group at C-6 on Ery and the exocyclic amine on A2062 (Fig. 4*A*). Notably, in the complex of Ery with the large ribosomal subunit of *Haloarcula marismortui*

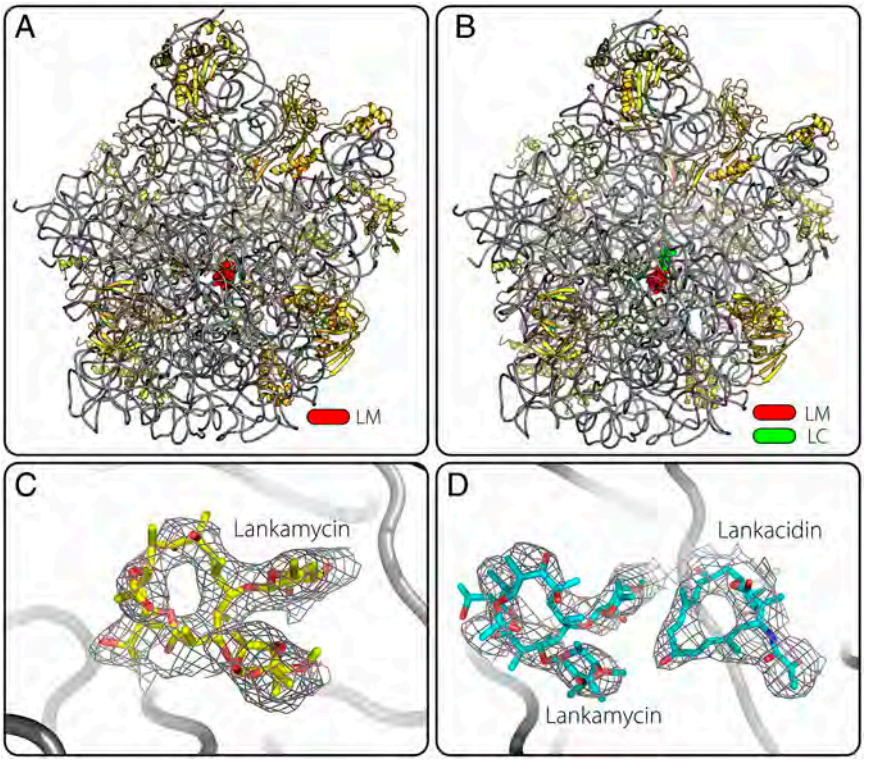

Fig. 2. (*A* and *B*) View of the entire ribosomal 50S structure, r proteins, and rRNA are drawn as cartoon ribbons, whereas the antibiotics are shown as spheres colored in red and green for lankamycin and lankacidin, respectively. (*A*) LM-D50S complex, (*B*) LM/LC-D50S complex, (*C* and *D*) enlargement of the binding regions shown in *A* and *B* with the $[2f_o - f_c]$ unbiased electron density map drawn at 1σ around the antibiotics, (*C*) LM-D50S complex, and (*D*) LM/LC-D50S complex (gray; surrounding rRNA backbone).

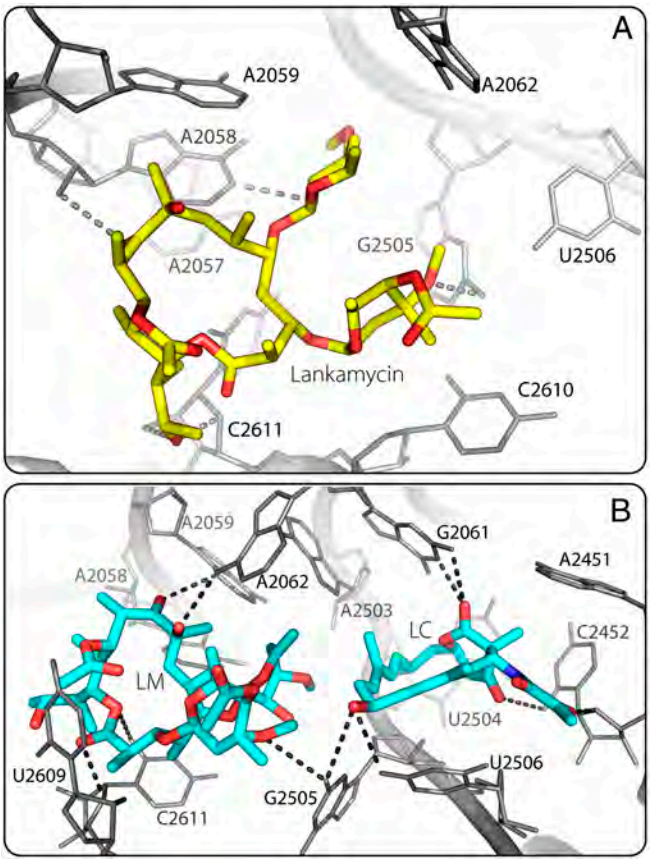

Fig. 3. Binding pockets of LM and LM/LC in the 50S subunit (dashed bonds indicate a hydrogen bond). (*A*) Interaction network of LM (yellow) with surrounding rRNA (gray). (*B*) Interaction network of LM and LC (cyan) with surrounding rRNA (gray).

(H50S) the conformation and position of A2062 are similar to those observed in the unbound ribosome (Fig. 4*C*).

Upon macrolide binding there is also a significant rearrangement of the position of C2610, a nucleotide that is located at the entrance to the exit tunnel. In its native conformation, C2610 would sterically clash with the macrolides (LM and Ery, Fig. 4*C*); however, in the presence of the antibiotics it moves away from the tunnel.

The [IC_{50}] of LM (Table 1) shows that compared to Ery it exerts a weaker inhibition of ribosomes by a few orders of magnitude (11). A comparison of the structures of LM-D50S complex with the Ery-50S complex (Fig. 3) shows that LM, although binding in the same binding pocket, does not benefit from two of Ery's main interactions, a hydrogen bond to A2062 and a salt bridge that Ery makes between its protonated amine on the desoamine sugar and the phosphate oxygen of G2505. This, coupled with the significant rRNA rearrangements occurring as a consequence of A2062 rotation rearrangements upon LM binding, yields insight as to the reasons for the weaker binding of LM to the 50S subunit compared to Ery.

LM/LC-D50S Binding Site. The structure of both the LM and LC in complex with the 50S subunit reveals that they bind in the same general sites that each uses when they are separately bound. LM binds in a similar manner, although it translates slightly closer to the PTC (~1 Å), whereas LC resides in an almost identical position (Figs. 2 and 3). Both antibiotics make similar contacts with the ribosome, contacting only rRNA or each other.

In its position within the LM/LC-D50S complex, LM maintains the hydrogen bond contacts between the ribose of C2611 as in the LM-D50S, but forms a hydrogen bond with endocyclic nitrogen in A2059 instead of A2058. The arcanose moiety also forms a new hydrogen bond between the acetate oxygen and U2586. A2062 is in a similar position as in the native D50S and Ery/D50S complex structures and forms a new hydrogen bond between the exocyclic amine and the hydroxyl group on C-8 of the macrolactone ring. Interestingly, G2505 forms a bridging hydrogen bond between the two antibiotics (Fig. 2*F*). There are also very similar hydrophobic interactions with surrounding bases within the binding pocket of LM being completed by A2058, A2503, U2609, and C2610.

In the double antibiotic/D50S complex structure, LC resides in almost exactly the same binding site as in its native LC-D50S complex (11). It makes hydrophobic contacts with A2451, C2452, U2504, and U2585 and hydrogen bonds with A2053, G2061, C2452, and U2506 (see Fig. 2*F*). There is also the bridging polar contact to LM mediated by G2505. LC binds in a well-defined Mg^{II} binding site (Fig. 3*B*), with the ketoamide group displacing the native position of the Mg^{II}, suggesting that the binding of this antibiotics is actually responsible in some manner for mediating the rRNA stability in this region.

Binding of LC into the PTC also induces coordinated changes in the positions of several rRNA nucleotides. There is coordinated movement of U2585 and U2506 (Fig. 3*B*), wherein upon binding of LC, U2585 moves away from LC to avoid a steric collision. This movement induces a change in the position of U2506 as it is no longer sterically hindered by U2585; this movement is also confirmed by 23S rRNA footprinting studies (see below vide infra).

LC and LM also make multiple van der Waals contacts between them. The arcanose and chalcose rings of LM are within hydrophobic contacts with the conjugated section of the LC macrolactone ring. These interactions would not be achieved unless LM also moved closer to the PTC as it does in the double antibiotic structure.

23S rRNA Footprinting Studies. The structures of D50S-LM, and D50S-LM/LC are supported by previously published high-resolution chemical footprinting of the 23S rRNA of *D. radiodurans* in complex with the combinations of LM and LC (11). When added alone, LM protects A2059 and A2058 from DMS modification and U2609 from CMCT [1-cyclohexyl-(2-morpholinoethyl)carbodiimide metho-p-toluene sulfonate] modification in the same manner that Ery does. The crystallographic results confirm this observation, showing an overlap between Ery and LM positions (Fig. 4*A*). LC partially protects A2059 as in the case of LM, yet it causes a hypersensitive response to DMS modification on A2058. Curiously, neither A2058 nor A2059 are in the binding vicinity of LC, but drug binding in the region of the PTC and entrance to the exit tunnel desensitizes these bases from chemical cleavage. This may suggest that these bases are involved in an induced fit mechanism that confers protection. However, as so far there is no structural evidence for large rearrangement of these bases compared to the native conformations, it is more likely that any drugs binding in this region (PTC, exit tunnel) act as mainly as steric inhibitors for DMS or CMCT, disallowing chemical cleavage.

When in complex (LC/LM), modification of A2058 is weaker than when induced by LC alone. A similar intermediate effect has been observed for the flexible U2585. LM and Ery do not affect the accessibility of U2585, and LC alone shields U2585 from alterations. However, in complex with LM, this shielding is partially relieved.

U2585 is part of the LC binding pocket, situated in proximity of the LC ketoamide group. The Mg^{II} ion in the native D50S structure and in the complex D50S-LM creates a hydrogen bond with U2585 and is displaced by LC. This observation can also explain the solvent accessibility of U2585 as the Mg^{II} does not hinder modification by CMCT.

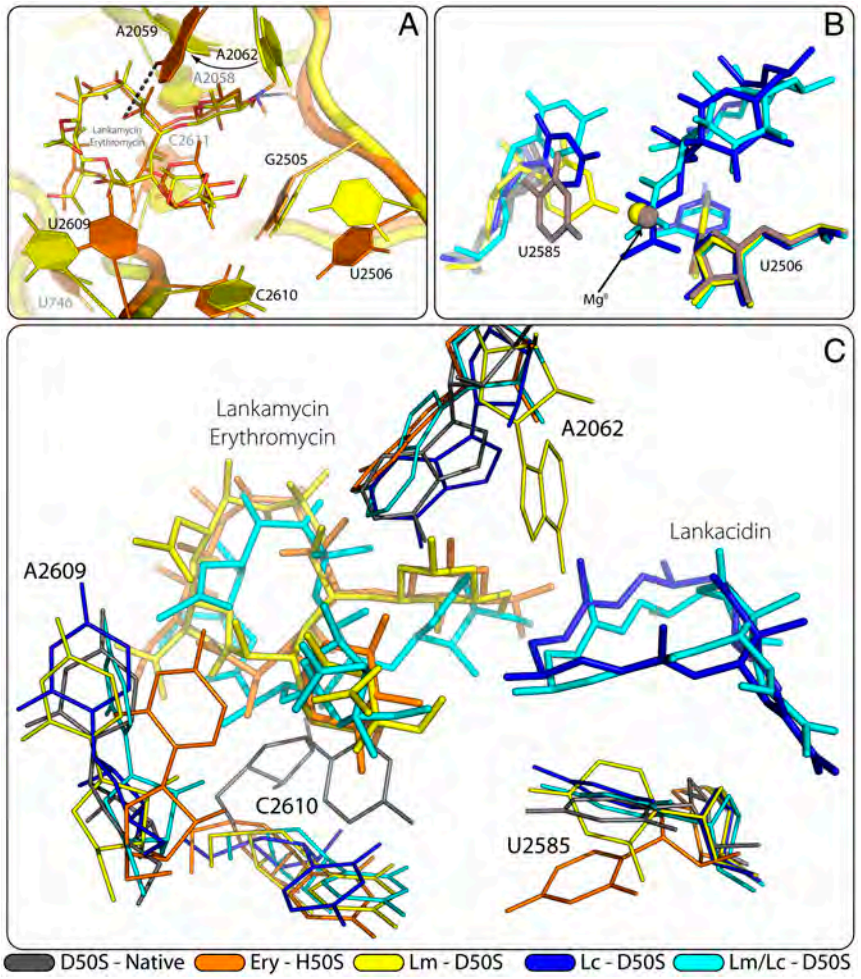

Fig. 4. (*A*) Structural overlay of binding site around Ery and LM {Ery-H50S complex [*1YI2* (12)] with Lankamycin-D50S complex (this work)}; note the shift of A2062 upon LM binding compared to its position in an empty subunit and to its position when Ery and LM/LC bind. (*B*) Structural overlay of the binding site around Lankacidin; the two bases that display correlated movement between the structures are shown. The two spheres are the position of Mg^{II} ions in the D50S and LM-D50S structures. [D50S-Native: *1NKW* (13); LM-D50S: this work; LC-D50S: *3JQ4* (11); LM/LC-D50S: this work]. (*C*) Overlay of the structures of various complexes of 50S with Erythromycin [H50S: *1YI2* (12); LM-D50S (this work); LC-D50S: *3JQ4* (11); and LM/LC-D50S (this work)]. Only selected nucleotides are shown for clarity.

Discussion

The crystallographic structures of the 50S ribosomal subunit in complex with LM as well as with LM with LC together give a clear indication as to their mechanisms for ribosomal inhibition. LM binds in the exit tunnel in a very similar manner to other members of the macrolide antibiotic family, essentially overlapping with the binding site of erythromycin (1, 2). Like other members of this family, LM action arises from physically blocking the progression of the nascent peptides through the tunnel. The binding site of LC in complex with LM is very similar to the previously reported D50S-LC structure, with drug binding in the PTC, preventing the proper placement of the aminoacyl end of the A-Site tRNA.

Table 1. Comparison of [IC_{50}] values for antibiotic inhibition of cell-free translation

Antibiotic	[IC_{50}] (μM)
Lankamycin (11)	275
Lankacidin (11)	1.5
Erythromycin (11)	0.2
Virginiamycin M (14)	0.8
Virginiamycin S (15)	2.5
Synercid™ (16)	~0.1

The synergistic behavior of LM/LC can possibly be explained by a few factors. LM is not a strong translation inhibitor, potentially owing to the steric hindrance of the methyl group at C-6 that hinders A2062 from forming a vital contact. However, the presence of LC in the PTC slightly rearranges the surrounding rRNA causing a slight repositioning of LM. This repositioning makes it possible for A2062 to bind to the lactone ring in LM, as well as for the positioning of the two antibiotics within hydrophobic interaction distance. It seems that A2062 is a vital base for the interactions between LM and LC. It has previously been reported that it is an extremely flexible nucleotide, serving as a "exit tunnel sensor" (17). It also appears to undergo significant movement upon its interactions with members of the streptogramin family (12, 18), potentially also mediating their synergistic ribosomal inhibition.

A comparison of the structural overlay of another synergetic pair of Streptogramins Synercid™: Quinupristin and Dalfopristin, clearly shows that both components bind to a similar region of the ribosome. LM and Quinupristin (Qn) bind in the exit tunnel and LC and Dalfopristin (Dn) are located in the PTC (Fig. 5). In fact, there are many similarities in their modes of action; both make hydrophobic contacts with each other, both make bridging contacts with the same nucleotide (A2602 for Qn/Dn and G2505 for LM/LC), both bind the 50S subunit making contacts solely

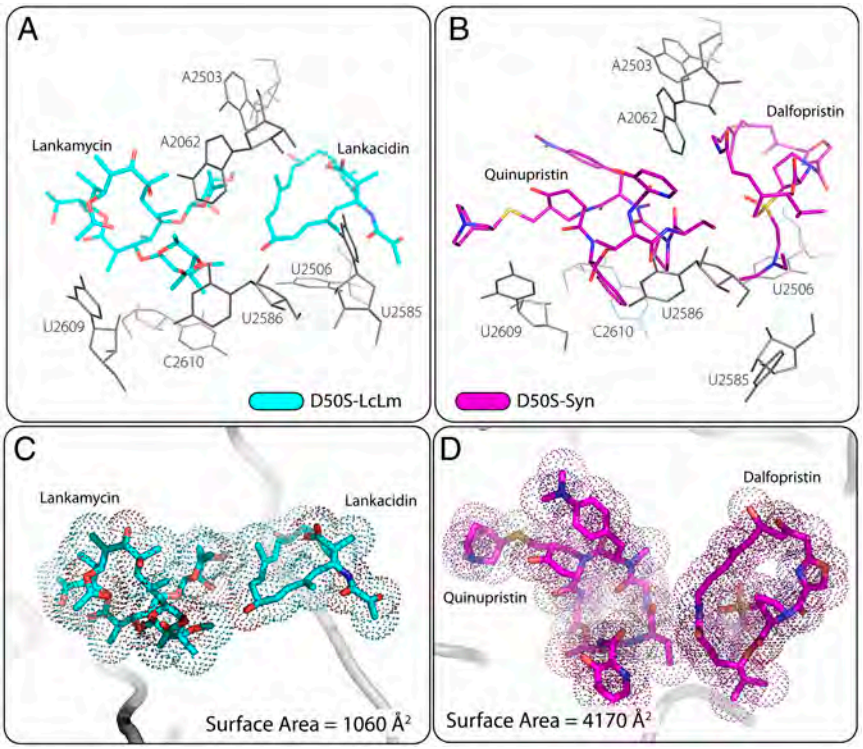

Fig. 5. Comparison of the binding of Synercid™: to the lankamycin/lankacidin pair. *A* and *B* are the same orientation and view of the PTC and exit tunnel region of the two structures [Synercid™: PDB ID code 1SM1 (18)]. (*C* and *D*) The calculated surface areas of both the LM/LC pair (*Left*) and the Synercid pair (*Right*).

with rRNA, and their binding is facilitated by an induced fit mechanism.

However, the Synercid™ combination is far more effective in ribosomal inhibition than the LM/LC pair (Table 1). First, Qn and Dn have a much larger van der Waals surface area (nearly 4 times that of the LM/LC combination, Fig. 5). This produces a much larger displacement in the rRNA, causing severe deleterious conformational changes (i.e., a 180° flip in U2585, Fig. 5). It has been shown that even after removal of Qn and Dn the affected cells have a lag time in recovery, most probably due to the extensive reorganization of their ribosomal internal structure (19, 20). Second, because of their more complex chemical nature (Fig. 1), they make substantially more contacts within their respective binding sites (18). Some insights are to be gained from these structural comparisons. The [IC_{50}] (11) values (Table 1) indicate that Synercid™ is significantly stronger than its family members (Virginiamycin S/M), possibly because its semisynthetic optimization that led to its relatively larger displacement size (Fig. 1). It seems that displacement size in this region of the ribosome plays a key role in ensuring ribosomal inhibition, as seen in the weaker inhibition by the LC/LM pair.

The relative size difference between Synercid™ and LC/LM accounts only partially for their respective synergistic behavior. It appears that in these two cases synergism arises from the antibiotics interactions with the ribosome, which involve conformational rearrangements, alongside the interactions with each other, resulting in an effect that is stronger than their arithmetically additive values. Thus, in both cases the binding of LC or Dn on the PTC components modulates the shape of the exit tunnel, allowing for tighter binding of the antibiotic partner, LM or Qn. This behavior was observed for streptogramins A and B (7), as well as for the LC/LM pair, particularly when comparing the three structures: D50S-LM, D50S-LC, and D50S-LC/LM, where the macrolide component enjoys more interactions with rRNA in the presence of LC. Moreover, in both cases the two components form hydrophobic interactions with each other (Fig. 5 *C* and *D*). This type of intermolecular interaction further anchors the antibiotics to their respective binding sites, while simultaneously lowering the degrees of freedom within the binding pocket.

Curiously, it seems that over the course of evolution two separate families of synergistic antibiotics have undergone convergent evolution to attack the same sites of the 50S subunit. Although it is clear that universal conclusions cannot be drawn from two cases, it is interesting that from two disparate starting points nature optimized simultaneous attack at very similar sites in the translation apparatus. From a drug discovery perspective, it highlights the importance of these two critical sites for future antibiotic leads. Modification of the macrolide component to further strengthen its binding may lead to more optimal synergetic combination.

Conclusions

The two structures of D50S-LM and D50S-LM/LC, supported by detailed chemical footprinting of 23S rRNA, show the binding sites of these antibiotics in the 50S ribosomal subunit and indicate that flexible nucleotides, such as A2062, may play a key role in drug binding. The stronger binding of LC aids the positioning of LM, thus allowing for synergistic inhibition of the ribosome, much in the same way as the Streptogramin A/B synergism. Although these drugs are not as effective as Synercid™, ideas for their development can be taken from the way Synercid™ was developed from virginiamycin M and S (Fig. 1), as well as from the valuable lessons derived from this study. It is also clear, at least in the two structures of synergistic antibiotics, that each of the synergistic drug components need to be within close proximity, as both structures reported thus far display interdrug hydrophobic contacts.

This work also may yield clues to the development of more potent 50S ribosomal interfering antibiotics. Enlargement of one or both of the components may lead to better synergism and more potent inhibition. Additionally covalent linkage of these

Table 2. Crystallographic data and refinement parameters

Parameters	LM-D50S	LM/LC-D50S
Crystals merged	4	8
Osc angle (φ°)	0.3°	0.2°
Beam line	ESRF 23-2	SLS-PXI
Detector	MARCCD-225	Pilatus-6M
Resolution (Å)	35–3.20 (3.31–3.20)	35–3.45 (3.57–3.45)
R_{merge} (%)	17.8 (71.3)	21.6 (85.7)
Completeness (%)	93.2 (34.0)	84.3 (85.6)
Redundancy	3.7 (2.2)	4.6 (4.5)
I/σ	7.1 (2.4)	5.6 (1.4)
Space group	*I*222	*I*222
Unit cell (Å)	a; 170.6	a; 169.7
	b; 410.2	b; 408.6
	c; 695.1	c; 693.3
R_{work}/R_{free} (%)	25.4/29.4	23.5/29.1
rmsd bonds, (Å)	0.01	0.01
rmsd angles, (°)	1.1	1.3

two drugs could lead to a powerful single molecule inhibitor that simultaneously binds two crucial sites in the ribosome.

Materials and Methods

D50S subunits were isolated and crystallized as previously described by McLellan et al. (21). The crystals of the LM-D50S complex were soaked in a solution of Hepes (pH = 7.8 at 21 °C, 10 mM), $MgCl_2$ (15 mM), ammonium chloride (75 mM), ethanol (20% vol/vol), 2-ethyl-1,3-hexanediol (10% vol/vol), and LM (900 μM) for 6 h prior to flash freezing. Crystals of the LM/LC-D50S complex were grown in the presence of LM (400 μM) and were subsequently soaked in the same buffer conditions as above with LC (25 μM).

Diffraction data were collected using a highly collimated synchrotron X-ray beam, using thin slice phi oscillation scans. Data were processed using MOSFLM (22), HKL2000 (23), and CCP4 (24). Map tracing and phase and model refinements were performed using COOT (22), CNS (25, 26), and PHENIX (27). Densities for the antibiotics were located on standard Fourier difference maps as well as simulated annealed composite-omit maps. Chemical restraints for the antibiotics were prepared using the PRODRG server (28) (http://davapc1.bioch.dundee.ac.uk/prodrg/) and were fitted to the difference maps. Mg^{2+}, Na^{+}, and K^{+} ions were located manually by careful analysis of the Fourier difference map; no attempt was made to model discrete water molecules. The antibiotic interactions with the ribosome were examined using LigPlot (29), and all images were generated by PyMOL (30). Crystallographic refinement details can be seen in Table 2.

ACKNOWLEDGMENTS. We thank the ribosome group at the Weizmann Institute for participating in the experiments reported. We thank the kind assistance of Prof. Alexander Mankin for useful discussions and comments and Pfizer, Inc. for providing initial LC samples. Crystallographic data were collected at ID23-2 at the European Synchrotron Radiation Facility in Grenoble, France, and at PXI station at the Swiss Light Source, and we thank the staff of both facilities for excellent assistance. This work was supported by National Institutes of Health Grant GM34360 (to A.Y.), U19 AI56575 (to A.S.M.), and by the Kimmelman Center for Macromolecular Assemblies. A.Y. holds the Martin and Helen Kimmel Professorial Chair.

1. Schlünzen F, et al. (2001) Structural basis for the interaction of antibiotics with the peptidyl transferase centre in eubacteria. *Nature* 413:814–821.
2. Douthwaite S (2010) Designer drugs for discerning bugs. *Proc Natl Acad Sci USA* 107:17065–17066.
3. Karageorgopoulos DE, Falagas ME (2009) New antibiotics: Optimal use in current clinical practice. *Int J Antimicrob Ag* 34(Suppl 4):S55–62.
4. Manfredi R, Sabbatani S (2010) Novel pharmaceutical molecules against emerging resistant gram-positive cocci. *Braz J Infect Dis* 14:96–108.
5. Baudoux P, et al. (2010) Activity of quinupristin/dalfopristin against extracellular and intracellular Staphylococcus aureus with various resistance phenotypes. *J Antimicrob Chemother* 65:1228–1236.
6. Adaleti R, et al. (2010) Prevalence of phenotypic resistance of *Staphylococcus aureus* isolates to macrolide, lincosamide, streptogramin B, ketolid and linezolid antibiotics in Turkey. *Braz J Infect Dis* 14:11–14.
7. Moureau P, Di Giambattista M, Cocito C (1983) The lasting ribosome alteration produced by virginiamycin M disappears upon removal of certain ribosomal proteins. *BBA-Gene Struct Expr* 739:164–172.
8. Arakawa K, Sugino F, Kodama K, Ishii T, Kinashi H (2005) Cyclization mechanism for the synthesis of macrocyclic antibiotic lankacidin in *Streptomyces rochei*. *Chem Biol* 12:249–256.
9. Kinashi H, Mori E, Hatani A, Nimi O (1994) Isolation and characterization of linear plasmids from lankacidin-producing Streptomyces species. *J Antibiot* 47(12):1447–1455.
10. Suzuki T, Mochizuki S, Yamamoto S, Arakawa K, Kinashi H (2010) Regulation of lankamycin biosynthesis in Streptomyces rochei by two SARP Genes, srrY and srrZ. *Biosci Biotechnol Biochem* 74:819–827.
11. Auerbach T, et al. (2010) The structure of ribosome-lankacidin complex reveals ribosomal sites for synergistic antibiotics. *Proc Natl Acad Sci USA* 107:1983–1988.
12. Tu D, Blaha G, Moore PB, Steitz TA (2005) Structures of MLSBK antibiotics bound to mutated large ribosomal subunits provide a structural explanation for resistance. *Cell* 121:257–270.
13. Harms JM, et al. (2001) High resolution structure of the large ribosomal subunit from a mesophilic eubacterium. *Cell* 107:679–688.
14. Nyssen E, Di Giambattista M, Cocito C (1989) Analysis of the reversible binding of virginiamycin M to ribosome and particle functions after removal of the antibiotic. *BBA-Gene Struct Expr* 1009:39–46.
15. Chinali G, Nyssen E, Di Giambattista M, Cocito C (1988) Inhibition of polypeptide synthesis in cell-free systems by virginiamycin S and erythromycin. Evidence for a common mode of action of type B synergimycins and 14-membered macrolides. *BBA-Gene Struct Expr* 949:71–78.
16. Mabe S, Champney WS (2005) A Comparison of a New Oral Streptogramin XRP 2868 with Quinupristin-Dalfopristin Against Antibiotic-Resistant Strains of *Haemophilus influenzae, Staphylococcus aureus*, and *Streptococcus pneumoniae*. *Curr Microbiol* 51:363–366.
17. Vazquez-Laslop N, Thum C, Mankin AS (2008) Molecular mechanism of drug-dependent ribosome stalling. *Mol Cell* 30:190–202.
18. Harms JM, Schlunzen F, Fucini P, Bartels H, Yonath A (2004) Alterations at the peptidyl transferase centre of the ribosome induced by the synergistic action of the streptogramins dalfopristin and quinupristin. *BMC Biol* 2:4.
19. Nyssen E, Di Giambattista M, Cocito C (1989) Analysis of the reversible binding of virginiamycin M to ribosome and particle functions after removal of the antibiotic. *Biochim Biophys Acta* 1009:39–46.
20. Parfait R, Cocito C (1980) Lasting damage to bacterial ribosomes by reversibly bound virginiamycin M. *Proc Natl Acad Sci USA* 77(9):5492–5496.
21. McLellan TJ, et al. (2009) A systematic study of 50S ribosomal subunit purification enabling robust crystallization. *Acta Crystallographica, Section D: Biological Crystallography DActa Crystallogr D* 65:1270–1282.
22. Leslie AGW (1992) Recent changes to the MOSFLM package for processing film and image plate data. *Joint CCP4 + ESF-EAMCB Newsletter on Protein Crystallography*, 26.
23. Otwinowski Z, Minor W, eds. (1997) *Processing of X-ray diffraction data collected in oscillation mode* (Academic, New York), 276, pp 307–326.
24. Collaborative Computational Project N (1994) The CCP4 Suite: Programs for protein crystallography. *Acta Crystallogr D* 50:760–763.
25. Brunger AT, et al. (1998) Crystallography & NMR System (CNS). *Acta Crystallogr D* 54:905–921.
26. Brunger AT (2007) Version 1.2 of the crystallography and NMR system. *Nat Protoc* 2:2728–2733.
27. Adams PD, et al. PHENIX: A comprehensive Python-based system for macromolecular structure solution. *Acta Crystallogr D* 66:213–221.
28. Schuettelkopf AW, van Aalten DMF (2004) PRODRG—A tool for high-throughput crystallography of protein-ligand complexes. *Acta Crystallogr D* 60:1355–1363.
29. Wallace AC, Laskowski RA, Thornton JM (1995) LIGPLOT: A program to generate schematic diagrams of protein-ligand interactions. *Protein Eng* 8:127–134.
30. Delano WL (2002) *The PyMOL Molecular Graphics System* (DeLano Scientific, Palo Alto, CA).